J. Phys. B: At. Mol. Opt. Phys. **30** (1997) 1785–1798. Printed in the UK PII: S0953-4075(97)80012-0

Electron capture and multiple ionization in collisions of fast H^+ and He^{2+} ions with gallium atoms

K O Lozhkin, C J Patton, P McCartney, M Sant'anna, M B Shah, J Geddes and H B Gilbody

Department of Pure and Applied Physics, The Queen's University of Belfast, Belfast, UK

Received 3 December 1996, in final form 27 January 1997

Abstract. A crossed-beam technique incorporating time-of-flight analysis and coincidence counting of the collision products has been used to study electron capture, and pure ionization of ground-state gallium atoms in collisions with H^+ and He^{2+} ions. Cross sections leading to the formation of up to six-fold ionized gallium in electron capture and up to four-fold ionized gallium through pure ionization have been determined within the energy range 38–1440 keV amu^{-1}. Pure ionization rather than electron capture is found to provide the main contribution to Ga^{q+} formation over most of the energy range considered. A notable feature of the electron capture data is the dominance of the Ga^{2+} transfer ionization contribution which is believed to be indicative of the important role of Auger ionization processes. Calculations based on an independent electron model of ionization (which have provided a good description of our previous measurements in Fe and Cu) are shown to fit our measured pure ionization cross sections in Ga very satisfactorily. In the case of electron capture, when the model is modified to take some account of Auger ionization, Ga^{q+} formation is described reasonably for H^+ impact but with only limited success for He^{2+} impact.

1. Introduction

A detailed quantitative assessment of the various collision processes leading to the multiple ionization of heavy metal atoms is necessary for the accurate modelling of both astrophysical and fusion plasmas. The general role of such processes in impurity control and plasma diagnostics which are relevant to the design of next-step fusion devices has been summarized by Janev (1993). In previous work in this laboratory (Patton *et al* 1994, 1995, 1996, Shah *et al* 1995a, b, 1996a) we have used a crossed-beam technique incorporating time-of-flight analysis and coincidence counting of the collision products to study electron capture and ionization in collisions of H^+ and He^{2+} ions with Fe and Cu atoms within the energy range 38–1440 keV amu^{-1}. In these measurements, a specially developed oven source (Shah *et al* 1996b) was used to provide thermal energy beams of ground state $3p^6 3d^6 4s^2\ {}^5D_4$ Fe and $3p^6 3d^{10} 4s\ {}^2S_{1/2}$ Cu atoms. In the case of H^+ impact, cross sections ${}_{10}\sigma_{0q}$ for the one-electron capture processes

$$H^+ + X \rightarrow H + X^{q+} + (q-1)e \tag{1}$$

for $q = 1$–4 for Fe and $q = 1$–5 for Cu were determined. Here, $q = 1$ corresponds to a simple charge transfer while $q > 1$ corresponds to a transfer ionization where electron capture takes place simultaneously with multiple ionization of the target. In the case of He^{2+} impact, the corresponding cross sections, ${}_{20}\sigma_{1q}$ for one-electron capture and ${}_{20}\sigma_{0q}$ for

0953-4075/97/071785+14$19.50

two-electron capture leading to X^{q+} product ions with $q = 1$–7, were determined. Cross sections for the pure ionization processes

$$H^+ + X \rightarrow H^+ + X^{q+} + qe \tag{2}$$

and

$$He^{2+} + X \rightarrow He^{2+} + X^{q+} + qe \tag{3}$$

were also determined for $q = 1$–4 and $q = 1$–3 respectively. It was found that both the electron capture and ionization measurements could be satisfactorily described in terms of an independent electron model approximation which assumed that electron removal takes place primarily from the 4s and 3d subshells.

In the present work we have carried out similar studies of electron capture and ionization of ground state $3d^{10}4s^24p\,^2P_{1/2}$ Ga atoms in collisions with H^+ and He^{2+} ions within the energy range 35–1440 keV amu^{-1}. At the lower energies within this range, electron capture processes are expected to be important, while at the higher energies, pure ionization is expected to provide the main contribution to Ga^{q+} formation. The electron subshell structure of Ga is significantly different from both Fe and Cu and the extent to which our simple independent electron model (previously applied successfully to those targets) can also describe Ga^{q+} formation is also of interest.

2. Experimental approach

The apparatus, measurement and normalization procedure was similar to that used previously in this laboratory (cf Shah *et al* 1995b, Patton *et al* 1995) and only the essential features need be outlined briefly here.

A primary beam of momentum analysed H^+ or He^{2+} ions of the required energy was arranged to intersect (at right angles) the thermal energy beam of ground-state Ga atoms from our oven source (Shah *et al* 1996b) in a high-vacuum region. The slow Ga^{q+} ions and electrons formed in the crossed-beam region were extracted with high efficiency by a transverse electric field applied between two high-transparency grids and, after a further stage of acceleration, were separately counted by particle multipliers. Ga^{q+} ions in any particular charge state, q, were selectively identified and distinguished from background gas-product ions by time-of-flight analysis. The Ga^{q+} ions arising from electron-capture collisions could be identified by counting them in coincidence with the fast H atoms, He^+ ions or He atoms arising from the same events which were recorded (after charge analysis by electrostatic deflection) by a third particle multiplier located beyond the beam intersection region. The Ga^{q+} ions arising from both transfer ionization and pure ionization could be identified by counting them in coincidence with the electrons arising from the same events. Alternatively, the primary ion beam could be pulsed and the Ga^{q+} product ions extracted from the crossed-beam region by a delayed extraction pulse prior to identification by time-of-flight analysis.

A careful analysis of the Ga^{q+}–fast atom/ion and the Ga^{q+}–electron coincidence spectra (see figures 1 and 2) in the way described previously (cf Shah *et al* 1995b, Patton *et al* 1995) allowed determination of the separate cross sections, ${}_{10}\sigma_{0q}$, for one-electron capture by 80–720 keV amu^{-1} H^+ ions where $q = 1$–5, ${}_{20}\sigma_{1q}$ for one-electron capture by 38–360 keV amu^{-1} He^{2+} ions where $q = 1$–6 and ${}_{20}\sigma_{0q}$ for two-electron capture by 38–250 keV amu^{-1} He^{2+} ions where $q = 2$–6. In addition, the pure ionization cross sections, ${}_{10}\sigma_{1q}$, for 87–1440 keV amu^{-1} H^+ ions where $q = 1$–4 and ${}_{20}\sigma_{2q}$ for 44–300 keV amu^{-1} He^{2+} ions where $q = 1$–3 were determined. Our measured relative cross sections were normalized to

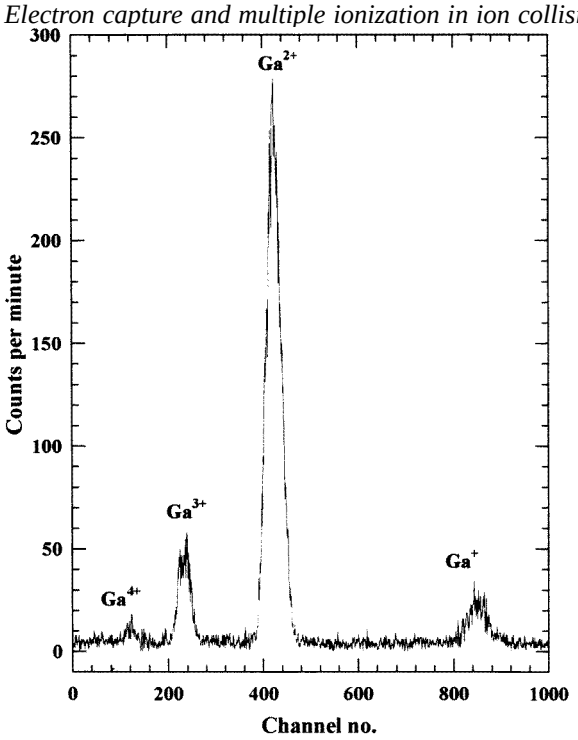

Figure 1. Fast H/slow Ga^{q+} ion time-of-flight coincidence spectrum resulting from one-electron capture by 125 keV H^+ ions in collisions with Ga atoms. Adjacent channel separation is 2 ns.

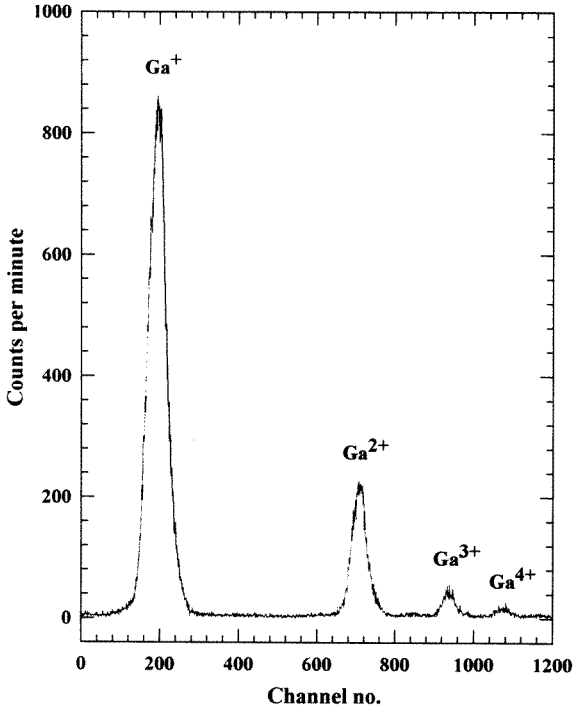

Figure 2. Slow Ga^{q+}/electron time-of-flight coincidence spectrum resulting from ionization of Ga atoms by 355 keV H^+ ions. Adjacent channel separation is 2 ns.

our previously measured cross sections (Patton *et al* 1996) for ionization of Ga by electron impact. This procedure, which has been described in detail previously (Shah *et al* 1992), involved the substitution of a pulsed primary ion beam by a pulsed beam of electrons while the target-beam conditions remained unchanged.

3. Results and discussion

3.1. Electron capture in collisions of H^+ and He^{2+} ions with Ga

Cross sections ${}_{10}\sigma_{0q}$ and ${}_{20}\sigma_{1q}$ for one-electron capture by H^+ and He^{2+} ions leading to Ga^{q+} formation are shown in tables 1 and 2 while cross sections ${}_{20}\sigma_{0q}$ for two-electron

Table 1. Cross sections ${}_{10}\sigma_{0q}$ for one-electron capture in H^+–Ga collisions leading to Ga^{q+} formation together with total electron capture cross sections σ_{10}.

Energy (keV amu^{-1})	σ_{10} (10^{-17} cm^2)	${}_{10}\sigma_{01}$ (10^{-17} cm^2)	${}_{10}\sigma_{02}$ (10^{-17} cm^2)	${}_{10}\sigma_{03}$ (10^{-18} cm^2)	${}_{10}\sigma_{04}$ (10^{-18} cm^2)	${}_{10}\sigma_{05}$ (10^{-19} cm^2)
80	12.3 ± 0.6	4.1 ± 0.4	7.3 ± 0.5	8.6 ± 0.7	0.78 ± 0.12	—
94	9.4 ± 0.5	2.0 ± 0.2	6.4 ± 0.5	8.6 ± 0.7	1.12 ± 0.12	—
108	7.5 ± 0.4	1.05 ± 0.09	5.5 ± 0.4	8.1 ± 0.6	1.24 ± 0.12	—
125	6.0 ± 0.4	0.54 ± 0.04	4.6 ± 0.4	7.0 ± 0.5	1.12 ± 0.12	2.5 ± 0.6
150	4.6 ± 0.4	0.27 ± 0.02	3.6 ± 0.3	6.3 ± 0.4	1.01 ± 0.12	2.6 ± 0.6
175	3.9 ± 0.3	0.16 ± 0.02	3.0 ± 0.3	5.8 ± 0.4	1.26 ± 0.12	3.2 ± 0.7
210	2.9 ± 0.2	0.08 ± 0.01	2.2 ± 0.2	5.2 ± 0.4	1.19 ± 0.12	1.5 ± 0.6
250	1.75 ± 0.09	0.05 ± 0.005	1.25 ± 0.08	3.5 ± 0.3	0.86 ± 0.10	1.6 ± 0.5
300	1.67 ± 0.09	0.03 ± 0.003	1.15 ± 0.08	3.8 ± 0.3	0.96 ± 0.09	1.8 ± 0.4
355	1.19 ± 0.06	0.02 ± 0.002	0.79 ± 0.06	2.9 ± 0.2	0.77 ± 0.08	1.8 ± 0.3
420	0.84 ± 0.05	—	0.55 ± 0.04	2.2 ± 0.2	0.58 ± 0.06	1.2 ± 0.2
500	0.54 ± 0.03	—	0.35 ± 0.03	1.52 ± 0.13	0.40 ± 0.04	0.55 ± 0.12
600	0.34 ± 0.02	—	0.22 ± 0.02	0.97 ± 0.08	0.22 ± 0.02	0.27 ± 0.04
720	0.20 ± 0.01	—	0.13 ± 0.01	0.57 ± 0.04	0.15 ± 0.02	—

Table 2. Cross sections ${}_{20}\sigma_{1q}$ for one-electron capture in He^{2+}–Ga collisions leading to Ga^{q+} formation together with total electron capture cross sections σ_{21}.

Energy (keV amu^{-1})	σ_{21} (10^{-16} cm^2)	${}_{20}\sigma_{11}$ (10^{-16} cm^2)	${}_{20}\sigma_{12}$ (10^{-16} cm^2)	${}_{20}\sigma_{13}$ (10^{-16} cm^2)	${}_{20}\sigma_{14}$ (10^{-17} cm^2)	${}_{20}\sigma_{15}$ (10^{-17} cm^2)	${}_{20}\sigma_{16}$ (10^{-17} cm^2)
38	29.4 ± 1.1	15.7 ± 0.9	9.6 ± 0.6	3.2 ± 0.3	7.9 ± 1.0	0.87 ± 0.16	—
44	24.2 ± 1.0	11.9 ± 0.8	8.2 ± 0.6	3.1 ± 0.3	10.0 ± 1.0	1.20 ± 0.15	—
53	17.3 ± 0.8	7.2 ± 0.5	6.2 ± 0.6	2.8 ± 0.3	9.8 ± 1.0	1.31 ± 0.15	—
63	13.9 ± 0.5	4.7 ± 0.3	5.5 ± 0.4	2.7 ± 0.2	8.9 ± 0.8	1.13 ± 0.20	—
75	9.9 ± 0.5	2.4 ± 0.2	4.2 ± 0.3	2.3 ± 0.3	8.0 ± 0.8	1.92 ± 0.31	0.31 ± 0.06
89	7.2 ± 0.4	1.15 ± 0.10	3.2 ± 0.3	1.85 ± 0.15	7.8 ± 0.6	1.80 ± 0.27	0.29 ± 0.05
105	5.6 ± 0.3	0.52 ± 0.07	2.6 ± 0.2	1.52 ± 0.13	7.0 ± 0.6	1.83 ± 0.24	0.34 ± 0.05
125	4.64 ± 0.19	0.23 ± 0.04	2.27 ± 0.15	1.28 ± 0.10	6.3 ± 0.5	1.87 ± 0.22	0.41 ± 0.05
150	3.72 ± 0.16	0.09 ± 0.02	1.82 ± 0.13	1.03 ± 0.08	5.5 ± 0.4	1.89 ± 0.20	0.38 ± 0.05
180	3.07 ± 0.14	0.04 ± 0.01	1.48 ± 0.11	0.86 ± 0.07	4.8 ± 0.3	1.74 ± 0.18	0.47 ± 0.05
212	2.53 ± 0.11	—	1.21 ± 0.08	0.71 ± 0.06	4.2 ± 0.3	1.53 ± 0.15	0.38 ± 0.04
250	2.22 ± 0.10	—	1.03 ± 0.08	0.63 ± 0.05	3.7 ± 0.3	1.51 ± 0.15	0.36 ± 0.03
300	1.80 ± 0.08	—	0.80 ± 0.06	0.53 ± 0.05	3.2 ± 0.2	1.23 ± 0.13	0.31 ± 0.03
360	1.47 ± 0.06	—	0.61 ± 0.04	0.42 ± 0.04	2.9 ± 0.2	1.22 ± 0.12	0.28 ± 0.03

Table 3. Cross sections ${}_{20}\sigma_{0q}$ for two-electron capture in He^{2+}–Ga collisions leading to Ga^{q+} formation together with total electron capture cross sections σ_{20}.

Energy (keV amu^{-1})	σ_{20} (10^{-17} cm^2)	${}_{20}\sigma_{02}$ (10^{-17} cm^2)	${}_{20}\sigma_{03}$ (10^{-17} cm^2)	${}_{20}\sigma_{04}$ (10^{-17} cm^2)	${}_{20}\sigma_{05}$ (10^{-18} cm^2)	${}_{20}\sigma_{06}$ (10^{-19} cm^2)
38	32.8 ± 2.0	6.2 ± 1.2	19.0 ± 1.4	7.6 ± 0.7	—	—
44	21.2 ± 1.3	2.5 ± 0.6	11.3 ± 1.0	6.3 ± 0.5	11.2 ± 1.7	—
53	17.6 ± 1.0	2.2 ± 0.4	9.0 ± 0.7	5.3 ± 0.5	11.3 ± 1.3	—
63	12.4 ± 0.4	1.4 ± 0.3	6.8 ± 0.7	3.4 ± 0.3	7.8 ± 0.8	—
75	6.7 ± 0.4	0.56 ± 0.09	3.3 ± 0.4	2.1 ± 0.2	7.7 ± 0.8	—
89	4.7 ± 0.4	0.28 ± 0.03	2.3 ± 0.2	1.5 ± 0.1	5.3 ± 0.5	8.0 ± 2.0
105	3.0 ± 0.2	0.10 ± 0.01	1.5 ± 0.1	1.0 ± 0.1	3.4 ± 0.3	8.0 ± 1.0
125	2.47 ± 0.15	0.09 ± 0.01	1.3 ± 0.1	0.74 ± 0.1	2.8 ± 0.3	6.0 ± 1.0
150	1.66 ± 0.12	0.04 ± 0.01	0.78 ± 0.06	0.57 ± 0.1	2.3 ± 0.2	4.2 ± 0.5
180	1.21 ± 0.06	0.03 ± 0.01	0.55 ± 0.04	0.42 ± 0.04	1.8 ± 0.2	3.3 ± 0.4
212	0.77 ± 0.04	—	0.33 ± 0.03	0.27 ± 0.02	1.5 ± 0.2	2.2 ± 0.3
250	0.57 ± 0.03	—	0.23 ± 0.02	0.20 ± 0.02	1.2 ± 0.1	2.0 ± 0.2

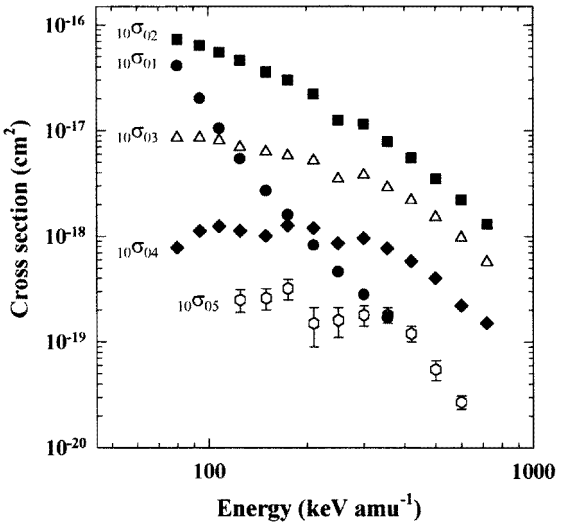

Figure 3. Cross sections ${}_{10}\sigma_{0q}$ for one-electron capture by H^+ ions in collisions with Ga atoms leading to Ga^{q+} formation.

capture by He^{2+} ions are shown in table 3. Total cross sections, $\sigma_{10} \approx \sum_{q=1}^{q=5} {}_{10}\sigma_{0q}$ and $\sigma_{21} \approx \sum_{q=1}^{q=6} {}_{20}\sigma_{1q}$, for one-electron capture and $\sigma_{20} \approx \sum_{q=2}^{q=6} {}_{20}\sigma_{0q}$, for two-electron capture are also included. The uncertainties associated with individual cross sections reflect 67% confidence levels based upon the degree of reproducibility of the measured values. In addition, all cross sections are subject to estimated uncertainties of 17% in absolute value as a result of our normalization to electron-impact data (Patton *et al* 1996).

Figure 3 shows the cross sections ${}_{10}\sigma_{0q}$ for one-electron capture by H^+ ions leading to Ga^{q+} ions for $q = 1$–5. Over the energy range considered, the transfer ionization cross section ${}_{10}\sigma_{02}$ leading to Ga^{2+} formation can be seen to provide the dominant contribution to σ_{10}. The cross section for simple charge transfer, ${}_{10}\sigma_{01}$, can be seen to be falling much more rapidly with increasing energy than ${}_{10}\sigma_{02}$. Indeed, the transfer-ionization contributions

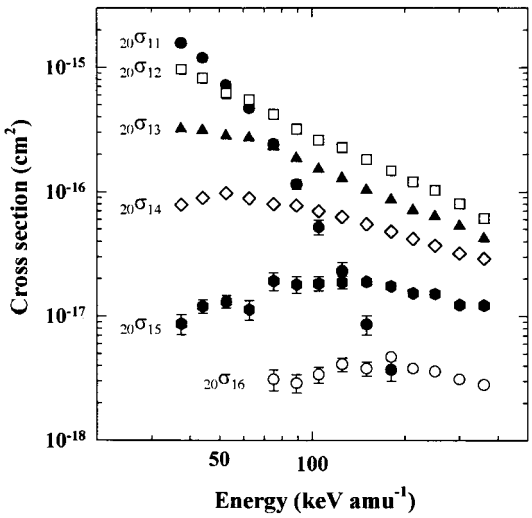

Figure 4. Cross sections $_{20}\sigma_{1q}$ for one-electron capture by He^{2+} ions in collisions with Ga atoms leading to Ga^{q+} formation.

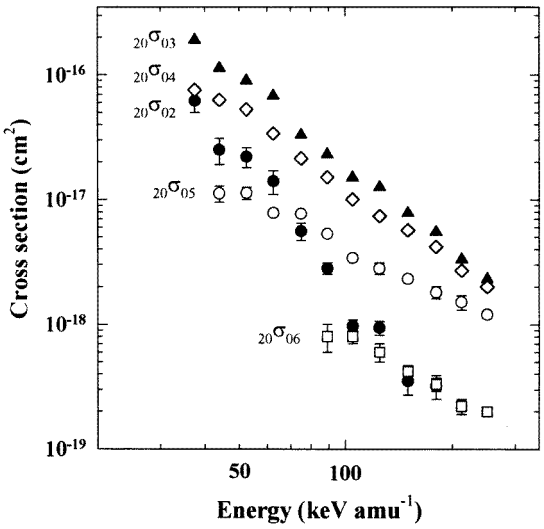

Figure 5. Cross sections $_{20}\sigma_{0q}$ for two-electron capture by He^{2+} ions in collisions with Ga atoms leading to Ga^{q+} formation.

from $_{10}\sigma_{03}$, $_{10}\sigma_{04}$ and $_{10}\sigma_{05}$ can be seen to exceed $_{10}\sigma_{01}$ at energies above about 120, 170 and 350 keV amu^{-1} respectively.

The cross sections for one-electron capture by He^{2+} ions (figure 4), which are limited to lower velocities, also show that the simple charge-transfer cross section, $_{20}\sigma_{11}$, is decreasing much more rapidly with increasing energy than the transfer ionization contribution $_{20}\sigma_{12}$ for Ga^{2+} production. The cross section, $_{20}\sigma_{11}$, is exceeded by $_{20}\sigma_{12}$ above about 60 keV amu^{-1}, and by $_{20}\sigma_{13}$, $_{20}\sigma_{14}$, $_{20}\sigma_{15}$, and $_{20}\sigma_{16}$ at energies which increase with q. In the case of two-electron capture by He^{2+} ions, the simple charge-transfer cross section, $_{20}\sigma_{02}$, decreases rapidly with increasing energy (figure 5) and is exceeded by both $_{20}\sigma_{03}$ and $_{20}\sigma_{04}$

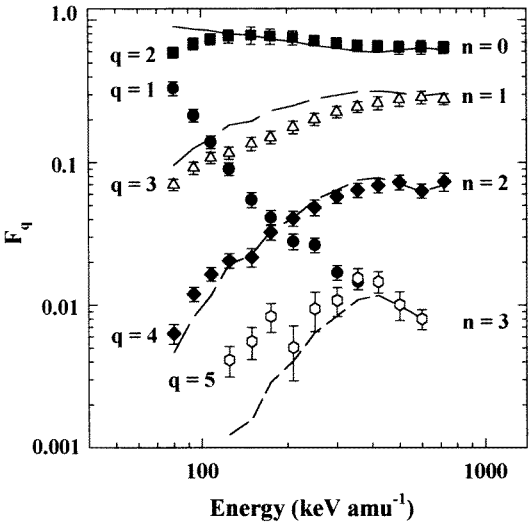

Figure 6. Measured charge-state fractions, F_q (shown as data points), for Ga^{q+} ions formed by one-electron capture in single collisions between H^+ ions and ground-state Ga atoms. Curves show calculated ionization probabilities, P_n, where $n = q - 2$ (see text) based on binomial distributions.

over the full extent of the present energy range and by ${}_{20}\sigma_{05}$ and ${}_{20}\sigma_{06}$ at energies above about 65 and 110 keV amu^{-1} respectively.

In the case of the transfer ionization processes, electron capture is accompanied by the removal of additional electrons from the outer subshells, the energy for which can be provided through binary type collisions. As in our previous studies of electron capture in Fe and Cu targets, it is interesting to try to describe the observed relative one-electron capture cross sections, ${}_{10}\sigma_{0q}$ and ${}_{20}\sigma_{1q}$, in terms of a model based on an independent electron description (cf McGuire 1991) of multiple ionization. Figures 6 and 8 show the energy dependence of our measured charge-state fractions, F_q, for Ga^{q+} ions formed by one-electron capture in single H^+–Ga and He^{2+}–Ga collisions respectively. At impact energies below those considered here, Ga^+ formation by simple charge transfer will primarily involve electron capture from the weakly bound outer 4p and 4s subshells. However, in the present energy range, capture of the more tightly bound 3d electrons would be expected to become significant due to closer matching of projectile and target electron orbital velocities. It is well known from studies of electron-impact ionization of Ga (see, for example, Vainshtein *et al* 1987) that removal of a 3d electron can result in many states through which Ga^{2+} formation occurs very effectively by autoionization. Such a process is consistent with the very large and weakly energy dependent values of F_2 observed here for both H^+ and He^{2+} impact.

In our previous measurements of electron capture in collisions with Fe and Cu (Patton *et al* 1994, Shah *et al* 1995b) it should be noted that, in the case of H^+ impact, while ${}_{10}\sigma_{01}$ also decreases more rapidly than ${}_{10}\sigma_{02}$, the relative rate of decrease is less than in the case of the present results for Ga. This seems likely to reflect the fact that capture of a 3d electron in Ga, unlike Fe and Cu, can lead to significant Auger ionization. In the case of He^{2+} impact, in addition to 3d electron capture, 3p capture is likely in Fe, Cu and Ga. However, while Auger ionization can only take place in Fe and Cu following 3p electron removal, it can occur in Ga following either 3p or 3d electron removal. This might account

for the relatively rapid decrease in ${}_{20}\sigma_{11}$ for Ga compared with the corresponding cross sections in Fe and Cu (Patton *et al* 1994, Shah *et al* 1995b). For two-electron capture, the fast decrease in ${}_{20}\sigma_{02}$ in Ga compared with the corresponding results for Fe and Cu (Patton *et al* 1994, Shah *et al* 1995b) may also be related to the relative likelihood of 3p or 3d electron captures followed by Auger ionization.

In our previous studies of electron capture in Fe and Cu we successfully described our observed values of F_q in terms of an independent electron model in which we express the probability of transfer ionization as a product of an electron capture probability, P_c, and an ionization probability, P_n, for the removal of n additional electrons from the target. In those cases, $n = q - 1$ for $q \geqslant 1$. However, in the present case of Ga where autoionization following one-electron capture is believed to result in a dominant Ga^{2+} contribution, it seems more appropriate to consider the number of electrons removed by ionization as $n = q - 2$. We can then use an analysis similar to that used previously. Thus cross section ${}_{10}\sigma_{01}$ may be expressed as

$$ {}_{10}\sigma_{0q} = 2\pi \int_0^\infty b P_c(b) P_n(b)\, \mathrm{d}b \tag{4} $$

where b is the impact parameter. Assuming $P_n(b)$ to be constant over the relatively small range of impact parameters where electron capture occurs then

$$ P_n = {}_{10}\sigma_{0q}/\sigma_{10} \tag{5} $$

where the total electron capture cross section $\sigma_{10} = \sum_q {}_{10}\sigma_{0q}$. Measured values of F_q can then be identified with P_n through (5).

The probability P_n that n electrons are ejected from either the 4p, 4s or 3d subshells can be estimated as detailed in our previous work (Shah *et al* 1995a) on the basis of binomial distributions which apply provided that it can be assumed that the probability for electron removal is the same for each subshell. A total of 12 electrons are available

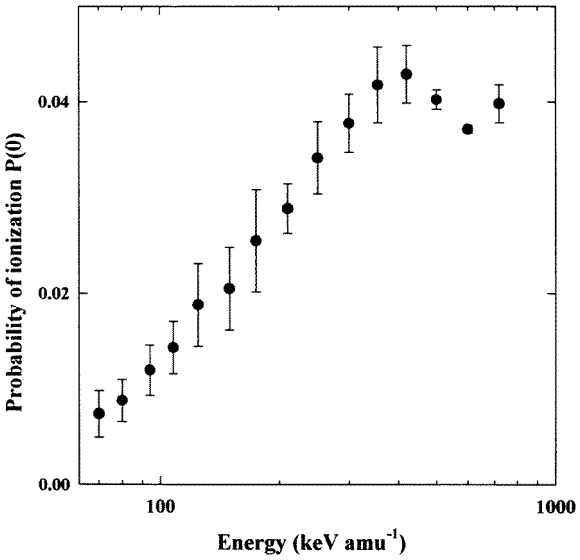

Figure 7. Ionization probabilities, $P(0)$, derived from binomial fits to measured charge-state distributions arising from one-electron capture by H^+ ions in collisions with Ga atoms.

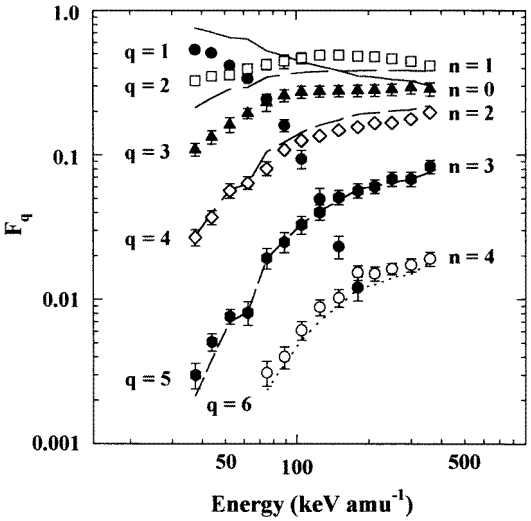

Figure 8. Measured charge-state fractions, F_q (shown as data points), for Ga^{q+} ions formed by one-electron capture in single collisions between He^{2+} ions and ground-state Ga atoms. Curves show calculated ionization probabilities, P_n, where $n = q - 2$ (see text) based on binomial distributions.

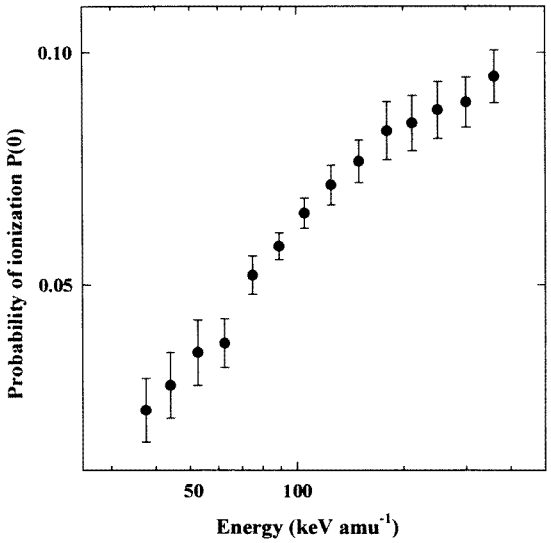

Figure 9. Ionization probabilities, $P(0)$, derived from binomial fits to measured charge-state distributions arising from one-electron capture by He^{2+} ions in collisions with Ga atoms.

from these subshells since the collisional ionization takes place much more rapidly than any autoionization process following one-electron capture.

At each energy in the present range, values of P_n (where $n = q - 2$) predicted in this way have been fitted (in figures 6 and 8) using a weighted least squares method to the measured fractions observed for both H^+ and He^{2+} impact while the corresponding energy dependence of the ionization probability for removal of a single electron from either the 3d,

4s or 4p subshells derived from the binomial fits are shown in figures 7 and 9. In the case of H^+ impact, the agreement between these predictions based on the binomial distribution and our measured fractions F_q for $q = 2$–5 can be seen (figure 6) to be in satisfactory general accord. The agreement with the curve for F_2 is unsatisfactory only at the lowest energies where $q = 1$ (not included in the model) becomes significant. In the case of the corresponding data for one-electron capture by He^{2+} ions (figure 8) there is good general agreement between the measured and calculated curves for $q = 4$, 5, 6. However, in the case of $q = 3$, 2, the fits are unsatisfactory. This poor agreement seems likely to reflect the fact that, in addition to 3d capture, capture of a 3p electron is also becoming significant. This will result in additional contributions to F_3 which are not taken account of in our simple model.

3.2. Pure ionization in collisions of H^+ and He^{2+} ions with Ga atoms

Our cross sections ${}_{10}\sigma_{1q}$ and ${}_{20}\sigma_{2q}$ for pure ionization of Ga by H^+ and He^{2+} impact leading to Ga^{q+} ions are shown in tables 4 and 5. The indicated uncertainties (at the 67% confidence level) reflect the degree of reproducibility of the individual cross sections. In addition, all cross sections are subject to an estimated additional uncertainty of 17% in absolute magnitude as a consequence of our normalization to electron impact data (Patton *et al* 1996).

Table 4. Cross sections ${}_{10}\sigma_{1q}$ for pure ionization of Ga by H^+ ions leading to Ga^{q+} formation.

Energy (keV amu^{-1})	${}_{10}\sigma_{11}$ (10^{-16} cm^2)	${}_{10}\sigma_{12}$ (10^{-17} cm^2)	${}_{10}\sigma_{13}$ (10^{-17} cm^2)	${}_{10}\sigma_{14}$ (10^{-18} cm^2)
87	14.2 ± 1.4	—	—	—
94	12.8 ± 1.1	—	—	—
105	12.0 ± 0.9	6.4 ± 1.2	0.78 ± 0.15	—
125	10.9 ± 0.7	8.9 ± 1.0	0.97 ± 0.15	—
150	9.6 ± 0.6	8.1 ± 0.8	1.07 ± 0.15	—
177	8.4 ± 0.5	8.5 ± 0.7	1.24 ± 0.14	1.6 ± 0.3
210	7.7 ± 0.5	9.0 ± 0.7	1.35 ± 0.14	1.5 ± 0.3
250	6.7 ± 0.6	9.1 ± 0.8	1.43 ± 0.14	1.9 ± 0.3
300	6.2 ± 0.4	8.7 ± 0.8	1.26 ± 0.13	1.9 ± 0.3
360	5.4 ± 0.3	8.5 ± 0.7	1.33 ± 0.13	1.8 ± 0.3
420	5.0 ± 0.3	8.4 ± 0.7	1.32 ± 0.13	2.0 ± 0.3
500	4.4 ± 0.3	8.4 ± 0.7	1.25 ± 0.12	1.5 ± 0.3
600	3.8 ± 0.2	7.5 ± 0.7	1.25 ± 0.12	1.7 ± 0.3
720	3.4 ± 0.2	6.9 ± 0.7	1.13 ± 0.12	1.9 ± 0.3
850	2.8 ± 0.2	6.1 ± 0.6	1.06 ± 0.10	1.4 ± 0.3
1000	2.6 ± 0.2	6.1 ± 0.5	0.99 ± 0.10	1.2 ± 0.2
1200	2.2 ± 0.2	5.4 ± 0.5	0.85 ± 0.09	1.2 ± 0.2
1440	2.0 ± 0.2	4.9 ± 0.5	0.77 ± 0.08	0.9 ± 0.2

Cross sections ${}_{10}\sigma_{1q}$ for pure ionization of gallium by H^+ impact are shown in figure 10. A comparison with the corresponding electron-capture data (figure 3) shows that Ga^+ formation is dominated by pure ionization over the energy range considered with cross sections ${}_{10}\sigma_{11}$ becoming very large and still rising at our low-energy limit. Pure ionization can also be seen to provide the main contribution to the formation of Ga^{2+}, Ga^{3+} and Ga^{4+} ions except at the lowest impact energies considered. The cross sections ${}_{10}\sigma_{12}$, ${}_{10}\sigma_{13}$ and ${}_{10}\sigma_{14}$ all pass through flat maxima within the range considered and decrease by less than an

Table 5. Cross sections ${}_{20}\sigma_{2q}$ for pure ionization of Ga by He^{2+} ions leading to Ga^{q+} formation.

Energy (keV amu^{-1})	${}_{20}\sigma_{21}$ (10^{-16} cm^2)	${}_{20}\sigma_{22}$ (10^{-16} cm^2)	${}_{20}\sigma_{23}$ (10^{-17} cm^2)
44	46.4 ± 3.7	1.1 ± 0.3	—
53	41.8 ± 3.1	0.9 ± 0.3	—
63	40.7 ± 3.0	1.4 ± 0.3	—
75	37.1 ± 2.8	1.4 ± 0.3	—
89	35.8 ± 2.8	2.3 ± 0.3	1.7 ± 0.6
105	31.5 ± 2.7	1.9 ± 0.3	2.4 ± 0.6
125	30.2 ± 2.8	1.9 ± 0.3	2.2 ± 0.6
150	24.2 ± 2.2	1.7 ± 0.2	2.2 ± 0.6
180	22.8 ± 2.1	1.8 ± 0.2	3.0 ± 0.5
213	22.5 ± 2.1	2.0 ± 0.2	3.8 ± 0.5
250	19.0 ± 1.7	1.7 ± 0.2	3.0 ± 0.5
300	17.5 ± 1.5	1.9 ± 0.2	3.8 ± 0.5

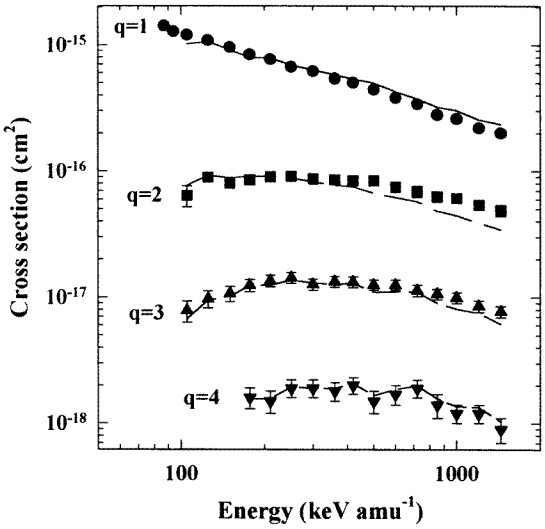

Figure 10. Measured cross sections for pure ionization, ${}_{10}\sigma_{1q}$ (shown as symbols), in collisions of H^+ ions with ground-state Ga atoms leading to Ga^{q+} formation compared with fits (shown as curves) based on an independent electron model of ionization.

order of magnitude as q increases.

The corresponding measurements for pure ionization in He^{2+}–Ga collisions are shown in figure 12. Again, a comparison with the electron capture data in figure 4 shows that Ga^+ formation is dominated by pure ionization with the cross section ${}_{20}\sigma_{21}$ becoming very large and still rising with decreasing energy at our low energy limit. In addition, Ga^{2+} and Ga^{3+} formation can be seen to take place primarily through pure ionization only at energies above about 150 keV amu^{-1} and beyond our maximum energy of 300 keV amu^{-1} respectively.

It is interesting to try to describe the present cross sections for pure ionization in terms of the same simple model based on an independent electron description of multiple ionization that we used in our studies of the multiple ionization of Fe and Cu (Patton *et al* 1995). We assume that the probability, P, for the removal of an electron from a particular subshell in

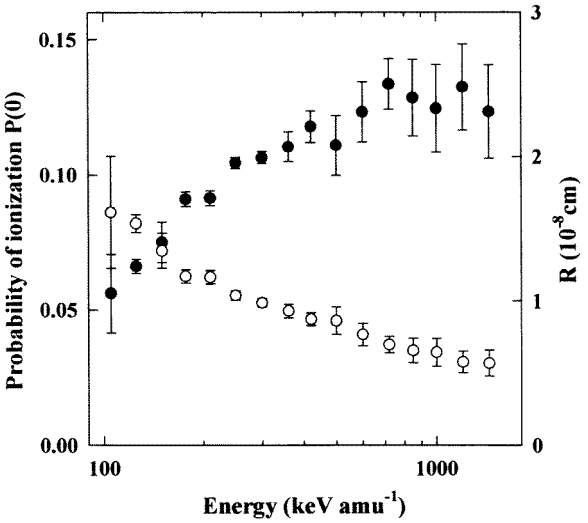

Figure 11. Plot showing the energy dependence of the fitting parameters, $P(0)$ (shown as ●), and R (shown as ○), in the expression for the ionization probability $P(b) = P(0)\exp(-b/R)$ for the ionization of Ga by H^+ ions.

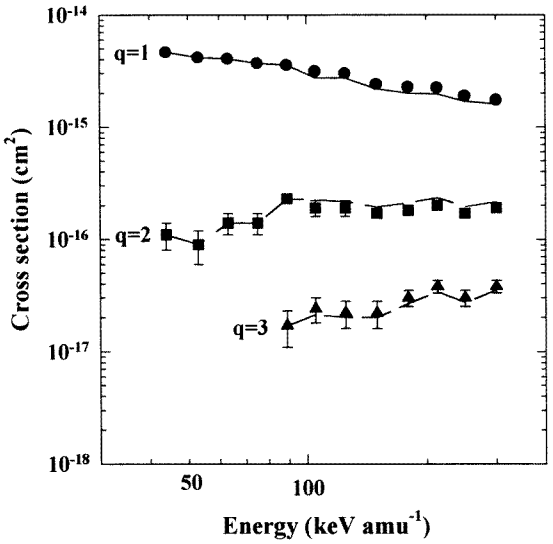

Figure 12. Measured cross sections for pure ionization, ${}_{20}\sigma_{2q}$ (shown as symbols), in collisions of He^{2+} ions with ground-state Ga atoms leading to Ga^{q+} formation compared with fits (shown as curves) based on an independent electron model of ionization.

the process of ionization can be approximated by the expression (see Matsuo *et al* 1994)

$$P(b) = P(0)\exp(-b/R) \tag{6}$$

where b is the impact parameter and $P(0)$ and R are constants for a particular subshell. As in our previous work, we make the simplest assumption that pure ionization primarily involves only the outermost subshells. For gallium these are the 4p, 4s and 3d subshells which contain 13 electrons. We also assume that the individual probabilities, $P(0)$, are the

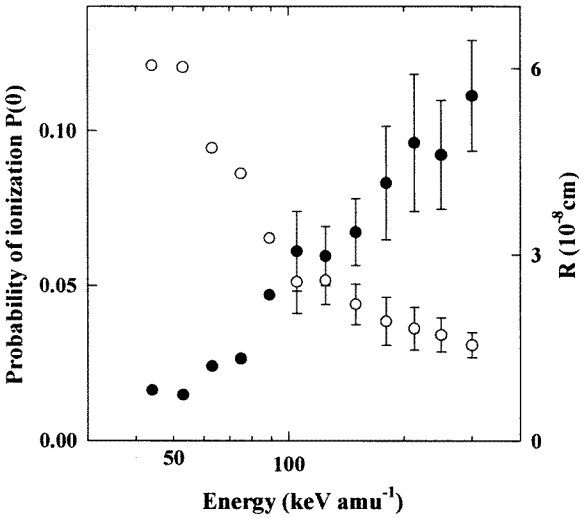

Figure 13. Plot showing the energy dependence of the fitting parameters, $P(0)$ (shown as ●), and R (shown as ○), in the expression for the ionization probability $P(b) = P(0)\exp(-b/R)$ for the ionization of Ga by He^{2+} ions.

same for each subshell. The cross sections for pure ionization resulting in the removal of q electrons from a total of N may then be described by the expression

$$\sigma = 2\pi \int_0^\infty \binom{N}{q} P(b)^q (1 - P(b))^{(N-q)} b \, \mathrm{d}b \tag{7}$$

where $\sigma = {}_{10}\sigma_{1q}$ or ${}_{20}\sigma_{2q}$ and $\binom{N}{q}$ is the binomial coefficient.

Values of ${}_{10}\sigma_{1q}$ or ${}_{20}\sigma_{2q}$ for pure ionization by H^+ and He^{2+} ions predicted by equation (7) have been fitted to our measured values using a weighted least-squares fit as in our previous work (Patton *et al* 1995). The result of this fit for H^+ impact (figure 10) can be seen to be very satisfactory. In the case of He^{2+} impact where the data are confined to lower velocities than for H^+ impact, the agreement (see figure 12) between the two sets of curves is also very satisfactory. The values of both $P(0)$ and R derived from the fitting procedure shown in figures 11 and 13 for H^+ and He^{2+} impact respectively exhibit an energy dependence very similar to that observed in our previous measurements for Fe and Cu (Patton *et al* 1995).

4. Conclusions

In this work we have studied, for the first time, electron capture and ionization in collisions of H^+ and He^{2+} ions with ground-state Ga atoms at energies within the range 35–1440 keV amu^{-1}. The separate cross sections for simple charge transfer, transfer ionization and pure ionization leading to up to six-fold ionized gallium have been obtained. In the energy range considered, Ga^+ production through pure ionization is dominant. Pure ionization rather than electron capture processes also dominate $q = 2$–4 formation by H^+ impact over most of the energy range considered. In the case of He^{2+} impact, $q = 2$, 3 formation takes place mainly by pure ionization at the higher energies considered. A notable feature of the present one-electron capture data, unlike the previous results for Fe and Cu, is the dominance of

the Ga^{2+} transfer ionization contributions which we believe is indicative of the important role of Auger ionization processes following 3d electron removal. An attempt to take some account of the latter by modifying the simple independent electron model previously applied to electron capture data for Fe and Cu is only partially successful. However, the model used previously to describe pure ionization of Fe and Cu has been fitted very satisfactorily to the present cross sections for pure ionization of gallium without any allowance for contributions from Auger processes.

Acknowledgments

This research forms part of a large programme supported by the Engineering and Physical Sciences Research Council. Two of us (CJP and PMcC) have been supported by Research Studentships from the Department of Education, Northern Ireland, while the visit of MS from Pontificia Universidade Católica do Rio de Janeiro was assisted by the IAESTE programme.

References

Janev R K 1993 Summary Report of IAEA Technical Committee Meeting on Atomic and Molecular Data for Fusion Reactor Technology, Cadarache, France *IAEA Report* INDC(NDS)-277, Vienna

Matsuo T, Tonuma T, Kumagai H and Tawara H H 1994 *Phys. Rev.* A **50** 1178

McGuire J H 1991 *Advances in Atomic, Molecular and Optical Physics* vol 29, ed D R Bates and B Bederson (New York: Academic) p 217

Patton C J, Bolorizahdeh M A, Shah M B, Geddes J and Gilbody H B 1994 *J. Phys. B: At. Mol. Opt. Phys.* **27** 3695

Patton C J, Shah M B, Bolorizahdeh M A, Geddes J and Gilbody H B 1995 *J. Phys. B: At. Mol. Opt. Phys.* **28** 3889

Patton C J, Lozhkin K O, Shah M B, Geddes J and Gilbody H B 1996 *J. Phys. B: At. Mol. Opt. Phys.* **29** 1409

Shah M B, McCallion P, Itoh Y and Gilbody H B 1992 *J. Phys. B: At. Mol. Opt. Phys.* **25** 3693

Shah M B, Patton C J, Geddes J and Gilbody H B 1995a *Nucl. Instrum. Methods Phys. Res.* B **98** 280

Shah M B, Patton C J, Bolorizahdeh M A, Geddes J and Gilbody H B 1995b *J. Phys. B: At. Mol. Opt. Phys.* **28** 1821

Shah M B, Patton C J, Geddes J and Gilbody H B 1996a *Am. Inst. Phys. Conf. Ser.* **362** 241

Shah M B, Bolorizadeh M A, Patton C J and Gilbody H B 1996b *Meas. Sci. Technol.* **7** 709

Vainshtein L A, Golovach D G, Ochkur V I, Rakovskii V I, Rumyantsev N M and Shustryakov V M 1987 *Sov. Phys.–JETP* **66** 36